Generation mechanism of electrostatic solitary structures in the Earth's auroral region

Q. M. Lu

School of Earth and Space Sciences, University of Science and Technology of China, Hefei, Anhui, China

D. Y. Wang

Purple Mountain Observatory, Chinese Academy of Sciences, Nanjing, Jiangsu, China

S. Wang

School of Earth and Space Sciences, University of Science and Technology of China, Hefei, Anhui, China

[1]   Satellite observations have revealed electrostatic solitary structures in the Earth's auroral region. These structures have positive electrostatic potentials and move along the ambient magnetic field. In this paper we performed one-dimensional electrostatic particle simulations of electrostatic solitary waves (ESW) in plasma composed of three electron components: cold, hot, and beam electrons. First, the nearly monochromatic electrostatic acoustic waves are excited. When the amplitude of the electron acoustic (EA) waves is sufficiently large, part of hot and beam electrons are trapped by the electron acoustic waves. These waves coalesce each other during their nonlinear evolution, and at last the solitary structures with travel speed related to the beam velocity are formed at the quasi-equilibrium stage. These structures have positive potential signatures, and they seem to be stable. Electron density cavities for cold electron component are always accompanied with these structures. In addition, the corresponding electric fields have a bipolar structure, which has also been observed in the Earth's auroral region recently. The conditions for existence of such solitary structures are investigated through our simulations, and the comparisons between our simulated results and satellite observations in the Earth's auroral regions are also discussed.

Citation: Lu, Q. M., D. Y. Wang, and S. Wang (2005), Generation mechanism of electrostatic solitary structures in the Earth's auroral region, *J. Geophys. Res.*, *110*, A03223, doi:10.1029/2004JA010739.

1.   Introduction

[2]   Intense electric field noise along the auroral field line was observed first by OV1-10 spacecraft [*Heppner*, 1969] and was later studied by satellites of Hawkeye 1 and IMP 6 [*Gurnett and Frank*, 1977] and DE 1 [*Lin et al.*, 1984; *Gurnett and Inan*, 1988]. The presence of intense and impulsive broadband electrostatic noise (BEN) has also been revealed by the Viking satellite with its high temporal resolution of wave experiments in the low-density region along the auroral field lines, in the 2000 to 10,000 km altitude range [*Pottelette et al.*, 1988, 1990, 1999]. BEN is an impulsive emission with amplitude up to 100 mV/m, and its characteristic variation time is typically a few hundreds of milliseconds. The spectrum of wave power can extend from very low frequencies up to frequencies much greater than the generally assumed local electron plasma frequency [*Dubouloz et al.*, 1991a]. In cold plasma theory no linear electrostatic wave mode is known in this frequency range Therefore BEN observed in the Earth's auroral

region is considered to relate to electrostatic solitary waves [*Dubouloz et al.*, 1991b; *Goldman et al.*, 1999]. Actually, large-amplitude solitary wave structures have recently been observed in this region. POLAR satellite observed such electrostatic solitary structures in the Earth's high-altitude polar magnetosphere [*Franz et al.*, 1998; *Tsurutani et al.*, 1998; *Cattell et al.*, 1999], and *Ergun et al.* [1998] reported FAST satellite observations of similar structures in downward current region of the midaltitude auroral zone. Generally, these structures have positively charged potentials and move along the ambient magnetic field. Their typical travel speed and parallel scale size are the order of 1000 km/s and 100 m, respectively. Most of the structures have isolated bipolar electric field with amplitude from several mV/m to hundreds of mV/m. There are two generation mechanisms for ESWs: electron acoustic solitary waves and BGK wave modes.

[3]   Electron acoustic solitary waves are nonlinear results when the amplitude of electron acoustic waves is sufficiently large. Electron acoustic waves exist in a two electron temperature plasma ("cold" and "hot" electrons). The hot to cold electron temperature ratio is larger than ∼10, and the hot electron component should represent a nonnegligible

fraction of the total electron density (more than ∼20%). The linear properties of electron acoustic waves have been investigated by many authors [*Tokar and Gary*, 1984; *Gary and Tokar*, 1985; *Mace and Hellberg*, 1990]. This wave mode exhibits an ion-acoustic like behavior in the sense that the cold and hot electrons play the roles of ions and electrons in the ion acoustic mode, respectively. The non-linear evolution of electron acoustic waves in an unmagnetized plasma has been studied by several authors with KdV or modified KdV equation [*Dubouloz et al.*, 1991b, 1993; *Mace and Hellberg*, 2001]. It is shown that electron acoustic waves can evolve into solitary structures when their amplitude is sufficiently large. However, the interpretation of the observed solitary structures in the auroral region in term of electron acoustic solitions in plasma composed of cold and hot electrons has been disregarded because such electron acoustic solitions were known to take the form of potential wells. The presence of an electron beam in the plasma allows the existence of electron acoustic solitions with potential humps [*Berthomier et al.*, 2000; *Wang*, 2003].

[4] The BGK wave modes are attributed to electron phase-space holes [*Bernstein et al.*, 1957; *Grabbe*, 2000], and the electron holes are created in waves from trapping of the electrons in the potential well. In order to explain the electrostatic solitary structures observed in the magnetotail [*Matsumoto et al.*, 1994], *Omura et al.* [1994, 1996] studied bistream and bump-on-tail instability with particle-in-cell simulations. The linear beam instability is first excited, and the electron phase-space holes are formed because part of electrons is trapped in waves. Then in a long nonlinear evolution, electron holes coalesce with adjacent holes and merge into larger, more intense holes, which at last lead to the formation of ESWs. The ESWs observed in the auroral region are thought to have the same generation mechanisms, which have been described in recent theoretical works [*Goldman et al.*, 1999, *Muschietti et al.*, 1999; *Newman et al.*, 2001; *Oppenheim et al.*, 2001; *Umeda et al.*, 2004].

[5] In this paper, with one-dimensional (1-D) electrostatic particle simulations, we investigate the nonlinear evolution of electron acoustic waves in a plasma system with three electron components: cold, hot, and beam electrons. Such a plasma system has already been studied by *Lin et al.* [1985] and *Matsukiyo et al.* [2004]; however, the nonlinear formation process of ESWs from electron acoustic waves has not been discussed before. The necessary condition for existence of such ESWs is also studied through changing the values of parameters.

[6] The organization of this paper is as follows. The simulation model is described in section 2. The 1-D particle simulation results of ESWs are presented in section 3. The comparisons between the simulation results and satellite observations in auroral zone are discussed in section 4, and a brief conclusion is also presented in section 4.

2. Simulation Model

[7] The present study employs a one-dimensional electrostatic particle-in-cell code. The model neglects the effect of magnetic field, and it only moves the electrons with the ions motionless [*Lu and Cai*, 2001]. In this model the electric fields and potentials are obtained by solving the Poisson equation, and the electrons move in the force of electric field.

Table 1. Simulation Parameters for Runs 1−7

Run	$\alpha = n_{h0}/n_{c0}$	$\beta = n_{b0}/n_{c0}$	$\theta = T_h/T_c$	$\varphi = T_h/T_b$	u_d/v_{Tc}
1	1.0	0.1	64.0	64.0	20.0
2	1.0	0.1	64.0	64.0	12.0
3	1.0	0.1	64.0	64.0	8.0
4	0.36	0.07	64.0	64.0	20.0
5	2.0	0.156	64.0	64.0	20.0
6	1.0	0.1	36.0	36.0	15.0
7	1.0	0.1	9.0	9.0	7.5

The periodic boundary conditions are used in the simulation model. In our simulations we consider a collisionless unmagnetized plasma system with three electron components (cold, hot, and beam electrons), and their initial velocity distributions are assumed to satisfy Maxwellian function: the cold and hot electrons are nondrifting Maxwellian, while the beam electrons are drifting Maxwellian. The initial densities of cold, hot, and beam electrons are n_{c0}, n_{h0}, and n_{b0}, respectively. Their corresponding temperatures (thermal velocities) are $T_c(v_{Tc})$, $T_h(v_{Th})$, and $T_b(v_{Tb})$. The beam velocity of beam electrons is u_d, and the total unperturbed density is $n_0 = n_{c0} + n_{h0} + n_{b0}$.

[8] Physical quantities are normalized as follows. The densities are normalized to the total unperturbed density n_0. The velocity is expressed in units of thermal velocity of cold electrons v_{Tc}. The space and time (x and t) are normalized to cold electron Debye length $\lambda_{Dc} = (\varepsilon_0 k_B T_c/n_{c0}e^2)^{1/2}$ and to the inverse of the total electron plasma frequency $\omega_{pe} = (n_0 e^2/m_e \varepsilon_0)^{1/2}$. The electric field and potential are normalized to $m_e \omega_{pe} v_{Tc}/e$ and $k_B T_c/e\varepsilon_0$.

[9] In the simulations, we use 1024 grid cells with the grid size $1.0\lambda_{Dc}$, and the time step is $0.02\omega_{pe}^{-1}$. There are 614,400 particles employed for each species of electrons. For convenience, we introduce the following quantities in our parametric study:

$$\alpha = \frac{n_{h0}}{n_{c0}}, \quad \beta = \frac{n_{b0}}{n_{c0}}, \tag{1}$$

$$\theta = \frac{T_h}{T_c}, \quad \varphi = \frac{T_h}{T_b}. \tag{2}$$

3. Simulation Results

[10] We have performed a set of simulations (runs 1−7) with different parameters, which are listed in Table 1. Figure 1 shows the time evolution of electric field energy $\varepsilon_p = \varepsilon_0 E_x^2/(2n_0 k_B T_c)$ in logarithmic scale for run 1. Here the electric field energy corresponds to the electrostatic waves excited by the beam electrons. It first passes through a linear growth stage and saturates at $\omega_{pe}t \sim 50.0$. Then the electric field energy begins to decrease until it reaches a quasi-equilibrium stage at $\omega_{pe}t \sim 1200.0$. The characteristics of waves excited in the linear growth stage and their nonlinear evolution for run 1 can be found in Figure 2, which shows the stacked profiles of the electric field in the x direction E_x. Figure 2a shows the stacked profiles of E_x during the period from $\omega_{pe}t = 36.0$ to $\omega_{pe}t = 50.0$, which corresponds to the linear growth stage. In this stage a nearly monochromatic electron acoustic wave mode is excited by the electron beam, and the wavelength and phase velocity are about
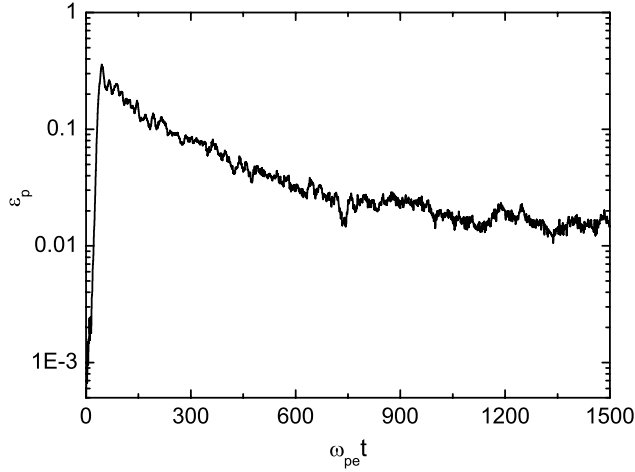
Figure 1. The time evolution of electric field energy $\varepsilon_p = \varepsilon_0 E^2/(2n_0 k_B T_c)$ in logarithmic scale (run 1).

$114.0\lambda_{Dc}$ and $13.5v_{Tc}$, respectively. According to the wavelength and phase velocity, we can calculate the frequency of the wave mode to be about $0.75\omega_{pe}$, which is nearly equal to the plasma frequency of cold electron component. Figure 2b describes the stacked profiles of E_x from $\omega_{pe}t = 132.0$ to $\omega_{pe}t = 160.0$, and the waves coalesce in this nonlinear evolution stage. It evolves from nine wavelengths

at $\omega_{pe}t = 132.0$ to seven wavelengths at $\omega_{pe}t = 160.0$. The solitary structures are formed through this continuing coalesce process, and at $\omega_{pe}t \sim 692.0$ two obvious solitons are formed. Figure 2c describes the process of the formation from two solitons to one single soliton. The solitons have bipolar electric structure, and Figure 2d shows the propagation of this single soliton. The travel speed of the soliton is about $18.3v_{Tc}$, which is related to the drift speed of the electron beam. From Figure 2d we also can find that this single soliton is a stable structure, which seems to exist forever. In summary, the ESWs are formed through coalesce of the nearly monochromatic waves excited in the linear growth stage. Their travel speed also increases in this coalesce process, and at last a single soliton is formed with the travel speed related to the beam velocity.

[11] Figure 3 describes the electric potential ψ, electric field E_x, beam electron density n_b, cold electron density n_c, and hot electron density n_h at $\omega_{pe}t = 1300.0$ for run 1. There is a compressive ESW at $x \sim 256.0\lambda_{Dc}$, and it is electric potential hump with scale size about $200\lambda_{DC}$. This structure has bipolar electric field with amplitude about $0.4m_e\omega_{pe}v_{Tc}/e$. It takes the form of a local increase of hot electron n_h and decrease of cold electron density n_c, and their relative variations are about 4% and 10%, respectively. For the beam electrons a large hump of electron density with relative variation about 40% is formed in the position of the soliton; however, an electron density cavity can be found at its center
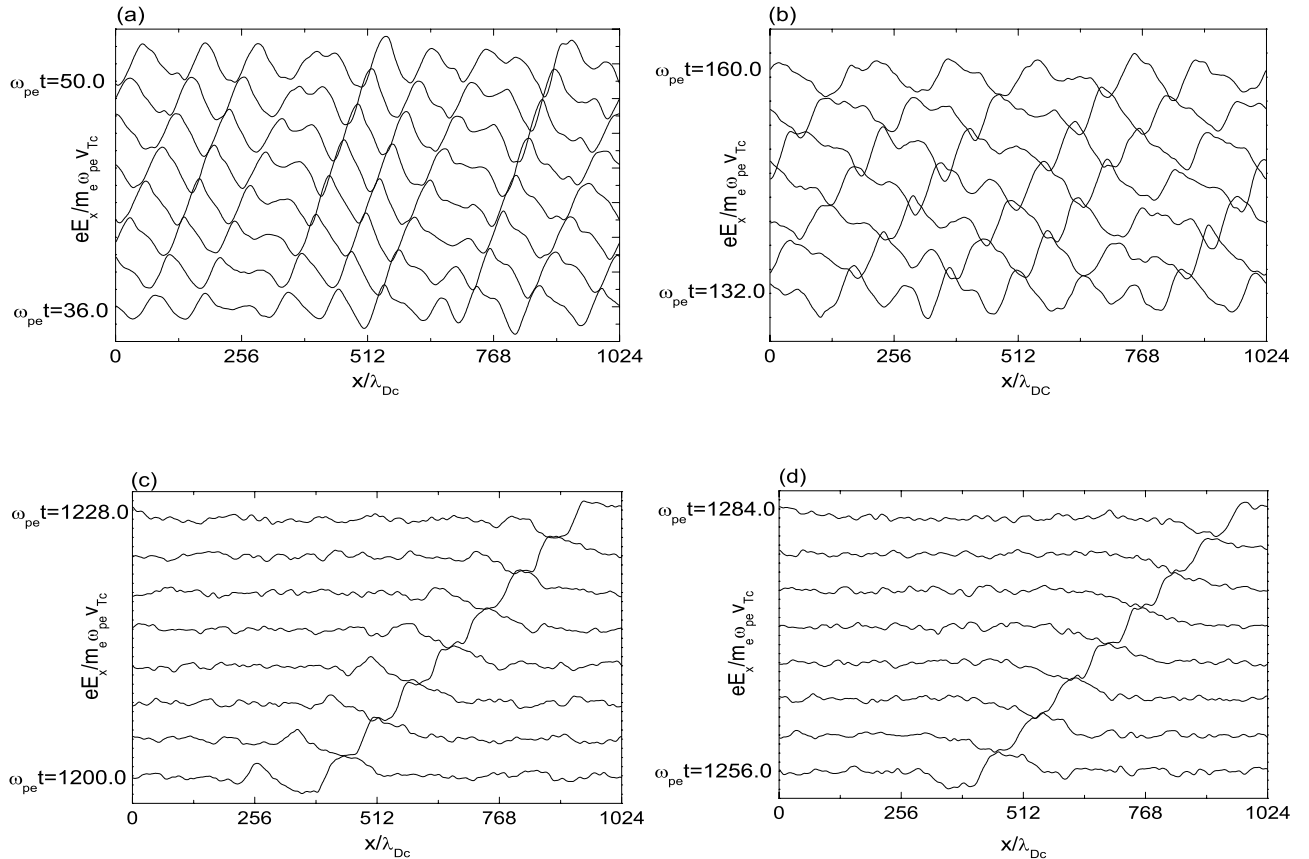
Figure 2. The stacked profiles of electric field in the x direction E_x during different time periods (run 1). (a) From $\omega_{pe}t = 36.0$ to $\omega_{pe}t = 50.0$, (b) from $\omega_{pe}t = 132.0$ to $\omega_{pe}t = 160.0$, (c) from $\omega_{pe}t = 1200.0$ to $\omega_{pe}t = 1228.0$, (d) from $\omega_{pe}t = 1256.0$ to $\omega_{pe}t = 1284.0$.
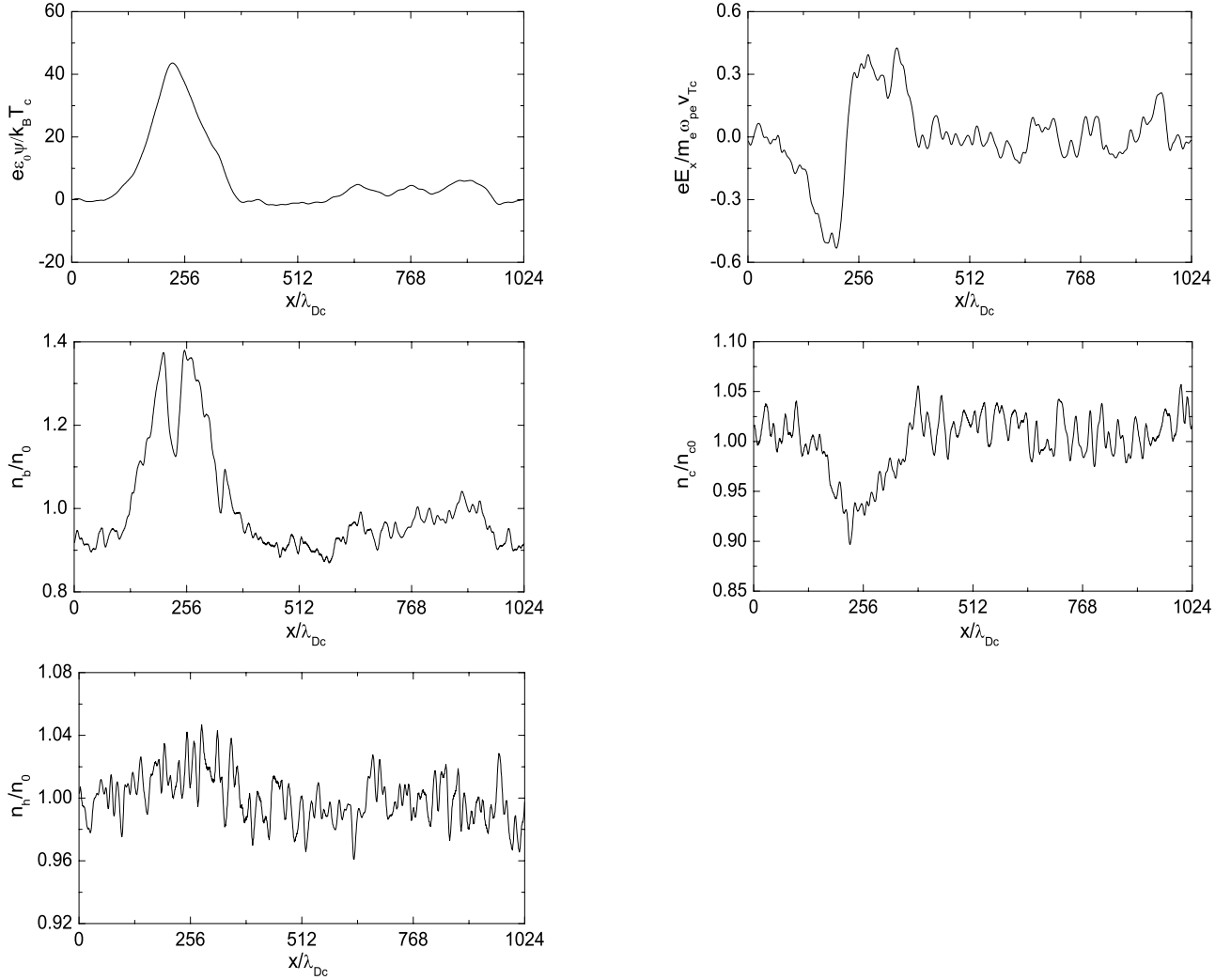
Figure 3. The spatial profiles of potential ψ, electric field E_x, beam electron density n_b, cold electron density n_c and hot electron density n_h at $\omega_{pe}t = 1300.0$ (run 1), which corresponds to the quasi-equilibrium stage.

with the relative variation about 20%. These density structures of the three electron components travel with the ESW, whose travel speeds are related to beam electron velocity. The $x - v_x$ phase diagram of the three electron components at $\omega_{pe}t = 1300.0$ for run 1 is shown in Figure 4. For the cold electrons the fluid velocity in the position of the ESW is negative, while for the beam and hot electrons, a phase-space hole can be found in the position of ESW. The electrons from the upstream and downstream of the ESW form such an electron hole, which is the signature of BGK wave modes.

[12] We can calculate the power spectrum of electric field E_x by Fourier transforming the electric field at a fixed spatial position, and Figure 5 shows the spectrum of E_x from $t = 1200.0\omega_{pe}^{-1}$ to $t = 1420.48\omega_{pe}^{-1}$ for run 1; this period is at the quasi-equilibrium stage. The spectral maximum is at about $0.45\omega_{pe}$; however, the spectrum can extend up to $3\sim4$ times of total electron plasma frequency. This is consistent with the satellite observations of Viking which the spectrum of BEN in auroral region can extend up to local electron plasma frequency [*Pottelette et al.*, 1990]. Of course the spectrum of solitary structures cannot explain

the whole spectrum of BEN in the auroral region, and parts of this spectrum are attributed to other physical factors.

[13] The important parameters for formation of ESWs are the beam electron velocity u_d, hot to cold electron density ratio α, and hot to cold electron temperature ratio θ. Figure 6 shows the electric field E_x and cold electron density n_c for run 2 and run 3. In run 2 and run 3 we change the beam electron velocity u_d, while keeping other parameters the same as run 1. In run 2 $u_d = 12.0v_{Tc}$, while in run 3 $u_d = 8.0v_{Tc}$. The ESWs only exist in run 2. The travel speeds are about $10.5v_{Tc}$, and their amplitudes are about $0.3m_e\omega_{pe}v_{Tc}/e$. Detailed analysis shows that the decrease of beam electron velocity can reduce the amplitude of ESWs, and ESWs only exist when the beam velocity is larger than about $10.0v_{Tc}$.

[14] Figure 7 describes the electric field E_x and cold electron density n_c for run 5 and run 6. In run 5 and run 6 we change the ratio of hot to cold electron density, while keeping the beam electron density $n_b = 0.05n_0$. In run 5, $\alpha = n_{h0}/n_{c0} = 0.36$ and $\beta = n_{b0}/n_{c0} = 0.07$. In run 6, $\alpha = n_{h0}/n_{c0} = 2.0$ and $\beta = n_{b0}/n_{c0} = 0.156$. Other parameters are same as
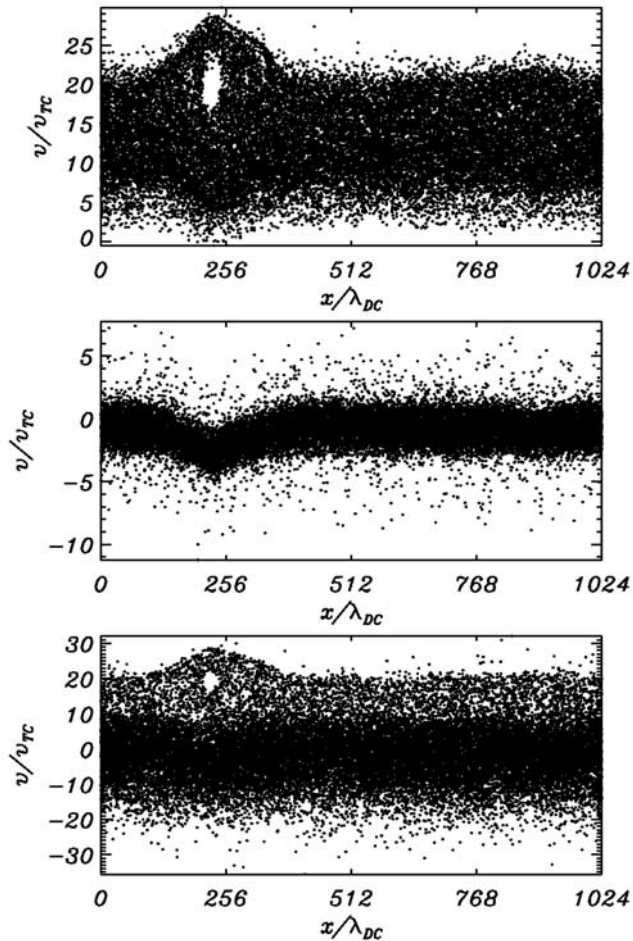
Figure 4. The $x - v_x$ phase diagram of electrons at $\omega_{pe}t = 1300.0$ (run 1) for (a) beam electrons, (b) cold electrons, (c) hot electrons.

run 1. The ESWs only exist in run 6 with travel speed about $19.5v_{Tc}$. Therefore another condition for existence of ESWs is sufficiently large hot to cold density ratio α, which is about 40%.

[15] Figure 8 describes the electric field E_x and cold electron density n_c for run 7 and run 8. In run 7 and run 8, we change the ratios of hot to cold and hot to beam electron temperature, while keeping u_d/v_{Th} as 2.5. In run 7, $\theta = T_h/T_c = 36.0$, $\varphi = T_h/T_b = 36.0$, and $u_d = 15v_{Tc}$. In run 8, $\theta = T_h/T_c = 9.0$, $\varphi = T_h/T_b = 9.0$, and $u_d = 7.5v_{Tc}$. Other parameters are same as run 1. There is an electrostatic soliton in run 7 with travel speed about $12.1v_{Tc}$, while no ESW exists in run 8. Therefore another condition for existence of ESWs is that the hot to cold temperature ratio θ is sufficiently large.

4. Summary and Discussions

[16] In this paper, using one-dimensional electrostatic particle simulations, we investigated the nonlinear evolution and properties of ESWs in an unmagnetized plasma composed of cold, hot, and beam electrons. *Lin et al.* [1985] and *Matsukiyo et al.* [2004] have also studied such plasma system with particle simulations. Lin et al. found the electron

acoustic mode is unstable in such plasma system, and the instability saturates by either trapping electrons or forming a plateau on the beam distribution. Matsukiyo et al. use much hotter beam electrons in their study. Their results showed that both the electron acoustic and electron two-beam (langmuir) instabilities are unstable. The electron two-beam waves are strong enough to have much higher growth rates and higher saturation levels than the electron acoustic wave. However, our study is focused on the nonlinear evolution of electron acoustic waves excited in such plasma system. At first a nearly monochromatic electron acoustic mode is excited by the beam electrons, and then in its nonlinear evolution the waves evolve into solitary structures through coalesces. At the same time the phase velocity of the waves increases in this process, and at last one or several stable solitary structures are formed at the quasi-equilibrium stage. Electron phase-space holes formed by trapping electrons can be found in the $x - v_x$ phase-space diagram (for hot and beam electrons). The properties of the solitary structures can be listed as follows: (1) the structures are compressive solitions with positive potential, (2) they have bipolar electric field structures, (3) their travel speeds are related to bulk velocity of beam electrons, (4) the power spectrum of the electric field can extend above the total electron plasma frequency and up to $3 \sim 4$ time of total electron plasma frequency, and (5) density cavities for cold electrons are always accompanied with these structures.

[17] These properties are similar to the electron acoustic solitary waves obtained by *Berthomier et al.* [2000] based on the KdV equation. The necessary conditions for existence of ESWs in such plasma system are also discussed in our simulations: sufficiently large beam electron velocity, hot to cold electron density, and temperature ratios.

[18] *Cattell et al.* [1999] reported the characteristics of solitary waves observed by Polar in the high-altitude cusp, and *Franz et al.* [1998] observed similar structures in the
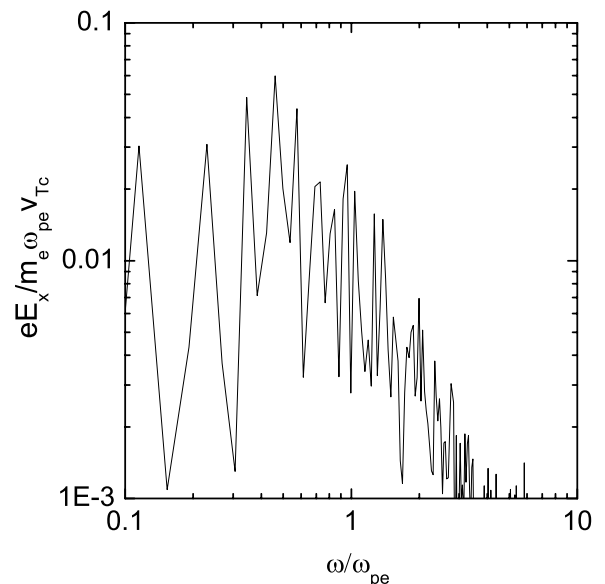

Figure 5. The power spectrum of electric field E_x for time $t = 1200.0 \sim 1420.48\omega_{pe}^{-1}$ (run 1), and the spectrum is obtained by Fourier transforming E_x at a fixed spatial position.
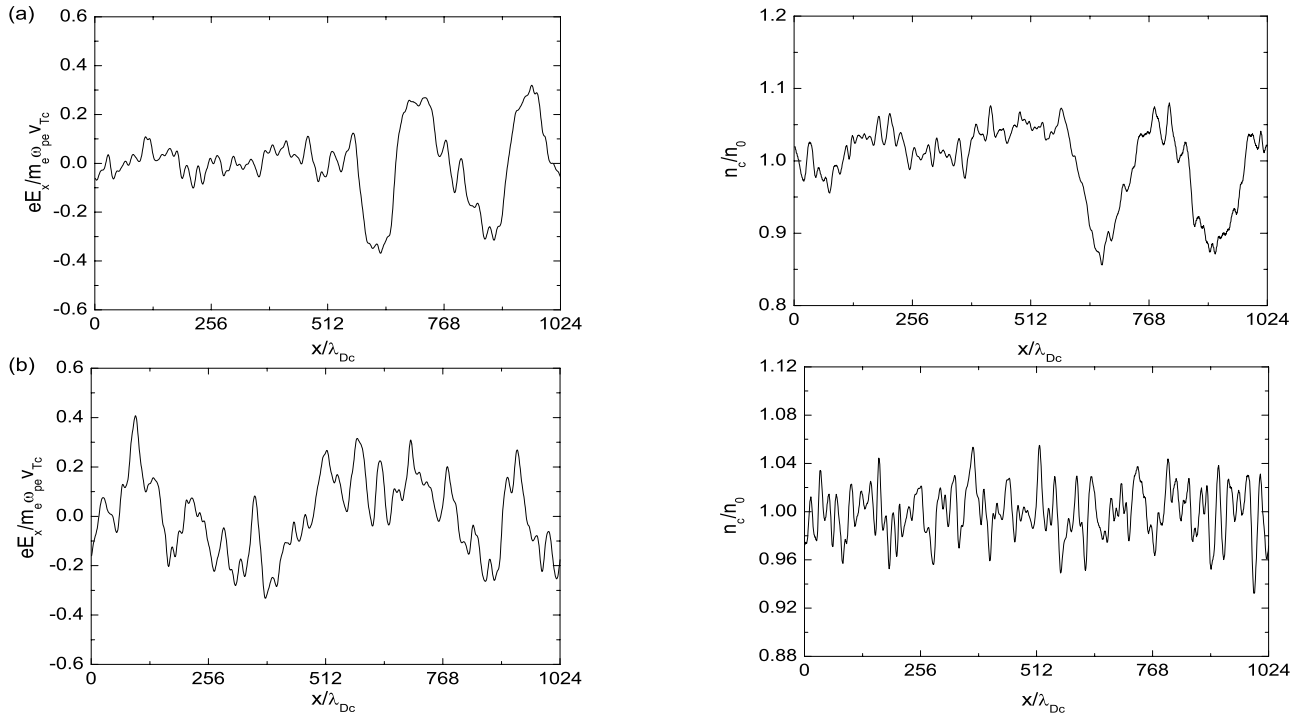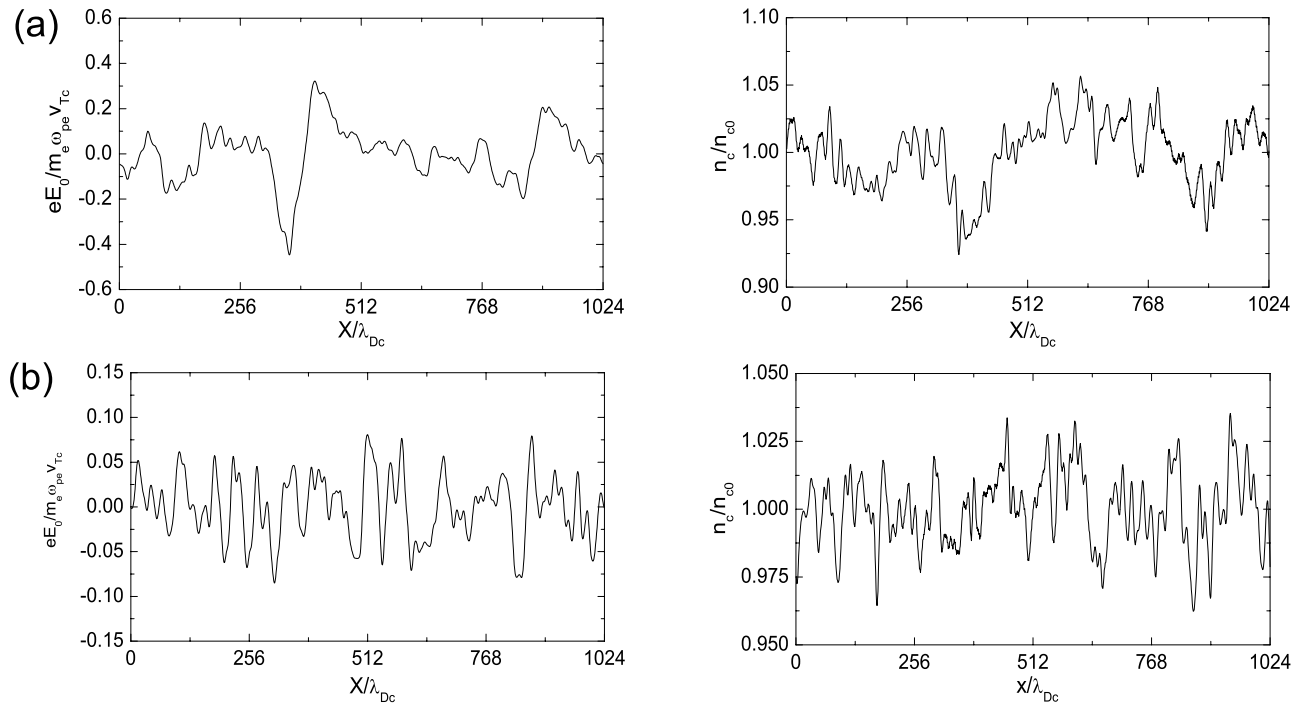
Figure 6. The spatial profiles of electric field E_x and cold electron density n_c for (a) run 2 and (b) run 3 at $\omega_{pe}t = 1300.0$, when the quasi-equilibrium stage has been reached.

high-altitude polar magnetosphere with the same satellite. These solitary waves, which have propagation speed the order of 1000 km/s, are positive potential structures with scale sizes about 1000 m, and they have bipolar electric structures. Similar structures are also observed in the low-altitude auroral zone [*Mozer et al.*, 1997; *Ergun et al.*, 1998], whose travel speed is up to ~5000 km/s, and amplitude of the electric field up to 2.5 V/m. These
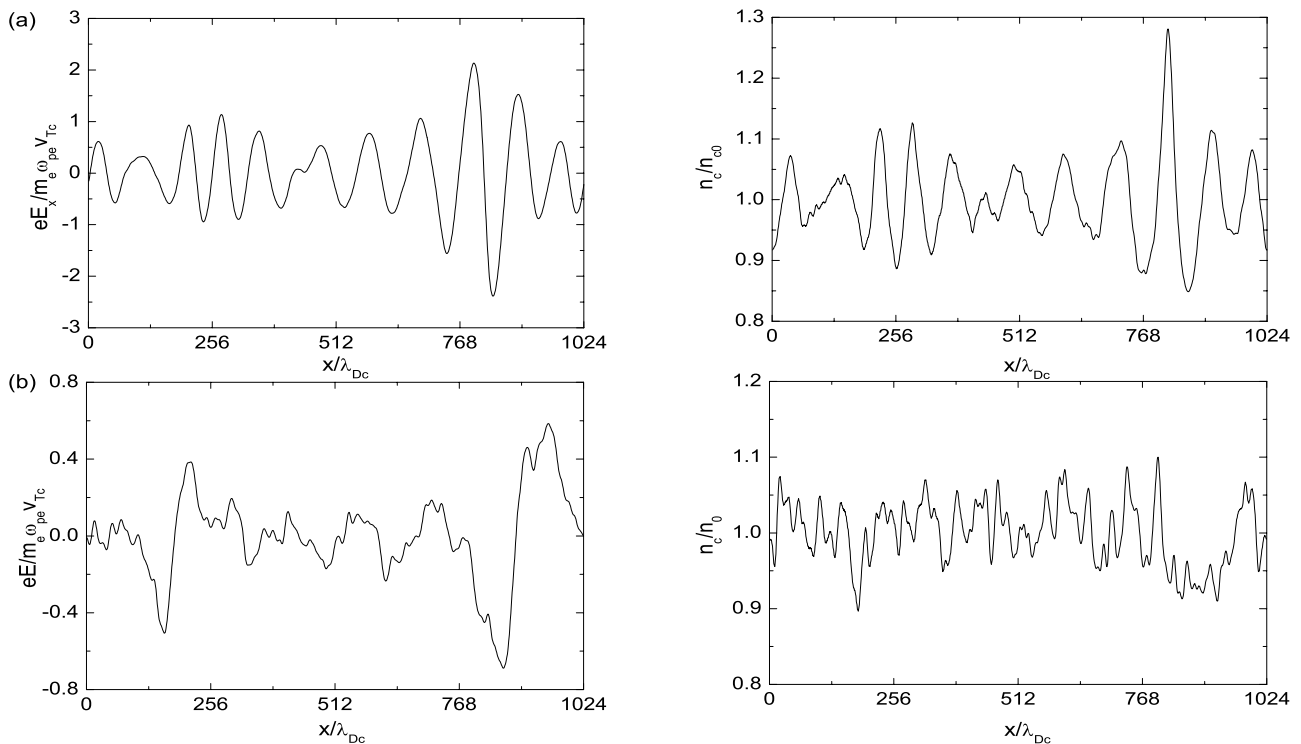
Figure 7. The spatial profiles of electric field E_x and cold electron density n_c for (a) run 4 and (b) run 5 at $\omega_{pe}t = 1300.0$, when the quasi-equilibrium stage has been reached.

Figure 8. The spatial profiles of electric field E_x and cold electron density n_c for (a) run 6 and (b) run 7 at $\omega_{pe}t = 2500.0$, when the quasi-equilibrium stage has been reached.

structures are very different from the type of solitary waves observed first in the auroral zone at low altitudes [*Temerin et al.*, 1982; *Bostrom et al.*, 1988], which have negative potential structures. In the auroral region the electron density are usually several electrons per cm^3, and the electron temperature is about several eV. In our simulations, for example run 1, the electric field amplitude, scale size, and travel speed of the solitary structure are about $0.4(m_e\omega_{pe}v_{Tc})/e$, $200\lambda_{Dc}$, and $19v_{Tc}$ respectively. We can easily find that they are roughly consistent with the observations. In summary, the beam electrons can excite electron acoustic waves in a three electron component plasma (cold, hot, and beam electrons), and it can evolve into electrostatic solitary structures. These structures have same characteristics as ESWs observed in the Earth's auroral region. However, our simulations neglect the effect of magnetic field. It has been found that the magnetic field may play an important role for ESWs [*Oppenheim et al.*, 1999], especially when the magnetic field is strong enough such as in the Earth's auroral region, which is the scope of our future investigation.

References

Bernstein, I. B., J. M. Greene, and M. D. Kruskal (1957), Exact nonlinear plasma oscillations, *Phys. Rev.*, *108*, 546–550.

Berthomier, M., R. Pottelette, M. Malingre, and Y. Khotyaintsev (2000), Electron-acoustic solitons in an electron-beam plasma system, *Phys. Plasmas*, *7*, 2987–2994.

Bostrom, R., et al. (1988), Characteristics of solitary waves and double layer in the magnetospheric plasma, *Phys. Rev. Lett.*, *61*, 82–85.

Cattell, C. A., J. Dombeck, J. R. Wygant, M. K. Hudson, F. S. Mozer, M. A. Temerin, W. K. Peterson, C. A. Kletzing, C. T. Russlell, and R. F. Pfaff (1999), Comparison of Polar satellite observations of solitary wave velocity in the plasma sheet boundary and the high altitude cusp to those in the auroral zone, *Geophys. Res. Lett.*, *26*, 425–428.

Dubouloz, N., R. Pottelette, M. Malingre, G. Holmgren, and P. A. Lindqvist (1991a), Detailed analysis of broadband electrostatic noise in the dayside auroral zone, *J. Geophys. Res.*, *96*, 3565–3579.

Dubouloz, N., R. Pottelette, M. Malingre, and R. A. Treumann (1991b), Generation of broadband electrostatic noise by electron acoustic solitons, *Geophys. Res. Lett.*, *18*, 155–158.

Dubouloz, N., R. A. Treumann, R. Pottelette, and M. Malingre (1993), Turbulence generated by a gas of electron acoustic solitons, *J. Geophys. Res.*, *98*, 17,415–17,422.

Ergun, R. E., et al. (1998), FAST satellite observations of large-amplitude solitary structures, *Geophys. Res. Lett.*, *25*, 2041–2044.

Franz, J. R., P. W. Kintner, and J. S. Pickett (1998), POLAR observations of coherent electric field structures, *Geophys. Res. Lett.*, *25*, 1277–1280.

Gary, S. P., and R. L. Tokar (1985), The electron acoustic mode, *Phys. Fluids*, *28*, 2439–2441.

Goldman, M. V., M. M. Oppenheim, and D. L. Newman (1999), Nonlinear two-stream instabilities as an explanation for auroral bipolar wave structures, *Geophys. Res. Lett.*, *26*, 1821–1824.

Grabbe, C. (2000), Generation of broadband electrostatic waves in the earth's magnetotail, *Phys. Rev. Lett.*, *84*, 3614–3617.

Gurnett, D. A., and L. A. Frank (1977), A region of intense plasma wave turbulence on auroral field line, *J. Geophys. Res.*, *82*, 1031–1050.

Gurnett, D. A., and U. S. Inan (1988), Plasma wave observations with the Dynamics Explorer 1 spacecraft, *Rev. Geophys.*, *26*, 285–316.

Heppner, J. P. (1969), Magnetospheric convection patterns inferred from high latitude activity, in *Atmospheric Emission*, edited by B. M. McCormac and A. Omholt, p. 251, Reinhold, New York.

Lin, C. S., J. L. Burch, S. D. Shawhan, and D. A. Gurnett (1984), Correlation of auroral hiss and upward electron beams near the polar cusp, *J. Geophys. Res.*, *89*, 925–935.

Lin, C. S., D. Winske, and R. L. Tokar (1985), Simulation of the electron acoustic instability in the polar cusp, *J. Geophys. Res.*, *90*, 8269–8280.

Lu, Q. M., and D. S. Cai (2001), Implementation of parallel plasma particle-in-cell codes on PC cluster, *Comput. Phys. Commun.*, *135*, 93–104.

Mace, R. L., and M. A. Hellberg (1990), Higher order electron longitudinal modes in a two electron temperature plasma, *J. Plasma Phys.*, *43*, 239–247.

Mace, R. L., and M. A. Hellberg (2001), The Korteweg-de Vries-Zakharov-Kuznetson equation for electron acoustic waves, *Phys. Plasmas*, *8*, 2649–2656.

Mamun, A. A., and P. K. Shukla (2002), Electron-acoustic solitary waves via vortex electron distribution, *J. Geophys. Res.*, *107*(A7), 1135, doi:10.1029/2001JA009131.

Matsukiyo, S., R. A. Treumann, and M. Scholer (2004), Coherent waveforms in the auroral upward current region, *J. Geophys. Res.*, *109*, A06212, doi:10.1029/2004JA010477.

Matsumoto, H., H. Kojama, T. Mayatake, Y. Omura, M. Okada, I. Nagano, and M. Tsutsui (1994), Electrostatic solitary waves (ESW) in the magnetotail: BEN wave forms observed by GEOTAIL, *Geophys. Res. Lett.*, *21*, 2915–2918.

Mozer, F., et al. (1997), New features in time domain electric field structures in auroral acceleration region, *Phys. Rev. Lett.*, *79*, 1281.

Muschietti, L., R. E. Ergun, I. Roth, and C. W. Carlson (1999), Phase-space electron holes along magnetic field lines, *Geophys. Res. Lett.*, *26*, 1093–1096.

Newman, D. L., M. V. Goldman, M. Spector, and F. Perez (2001), Dynamics and instability of electron phase-space tube, *Phys. Rev. Lett.*, *86*, 1239–1242.

Omura, Y., H. Kojama, and H. Matsumoto (1994), Computer simulation of electrostatic solitary waves: a nonlinear model of broadband electrostatic noise, *Geophys. Res. Lett.*, *21*, 2923–2926.

Omura, Y., H. Matsumoto, T. Miyake, and H. Kojama (1996), Electron beam instabilities as generation mechanism of electrostatic solitary waves in the magnetotail, *J. Geophys. Res.*, *101*, 2685–2697.

Oppenheim, M. M., D. L. Newman, and M. V. Goldman (1999), Evolution of electron phase-space holes in a 2D magnetized plasma, *Phys. Rev. Lett.*, *83*, 2344–2347.

Oppenheim, M. M., G. Vetoulis, D. L. Newman, and M. V. Goldman (2001), Evolution of electron phase-space electron holes in 3D, *Geophys. Res. Lett.*, *28*, 1891–1893.

Pottelette, R., M. Malinger, A. Bahnsen, L. Eliasson, K. Stasiewicz, R. E. Erlandson, and G. Marklund (1988), Viking observations of burst of intense broadband noise in the source regions of auroral kilometric radiation, *Ann. Geophys.*, *6*, 573–586.

Pottelette, R., M. Malingre, N. Dobouloz, B. Aparicio, R. Lundin, G. Holmgren, and G. Marklund (1990), High-frequency waves in the cusp/cleft regions, *J. Geophys. Res.*, *95*, 5957–5971.

Pottelette, R., R. E. Ergun, R. A. Treumann, M. Berthomier, C. W. Carlson, J. P. McFadden, and I. Roth (1999), Modulated electron-acoustic waves in auroral density cavities: Fast observation, *Geophys. Res. Lett.*, *26*, 2629–2632.

Temerin, M., et al. (1982), Observations of solitary waves and double layer in the auroral plasma, *Phys. Rev. Lett.*, *48*, 1175.

Tokar, R. L., and S. P. Gary (1984), Electrostatic hiss and the beam driven electron acoustic instability in the dayside polar cusp, *Geophys. Res. Lett.*, *11*, 1180–1183.

Tsurutani, B. T., J. K. Arballo, G. S. Lakhina, C. M. Ho, B. Buti, J. S. Pickett, and D. A. Gurnett (1998), Plasma waves in the dayside polar cap boundary layer: Bipolar and monopolar electric pulses and whistler mode waves, *Geophys. Res. Lett.*, *25*, 4117–4120.

Umeda, T., Y. Omura, and H. Matsumoto (2004), Two-dimensional particle simulation of electromagnetic field signature associate with electrostatic solitary waves, *J. Geophys. Res.*, *109*, A02207, doi:10.1029/2003JA010000.

Wang, D. Y. (2003), Electron-acoustic compressive soliton and electron density hole in aurora, *Chin. Phys. Lett.*, *20*, 533–536.

————————————

Q. M. Lu and S. Wang, School of Earth and Space Sciences, University of Science and Technology of China, Hefei, Anhui 230026, China. (qmlu@ustc.edu.cn)

D. Y. Wang, Purple Mountain Observatory, Chinese Academy of Sciences, Nanjing, Jiangsu 210008, China.